Deep-Sea Research II 104 (2014) 106–119

Contents lists available at ScienceDirect

Deep-Sea Research II

journal homepage: www.elsevier.com/locate/dsr2

Geomorphic characterization of four shelf-sourced submarine canyons along the U.S. Mid-Atlantic continental margin

Jeffrey Obelcz [a,*], Daniel Brothers [a], Jason Chaytor [a], Uri ten Brink [a], Steve W. Ross [b], Sandra Brooke [c]

[a] Woods Hole Coastal and Marine Science Center, US Geological Survey, 384 Woods Hole Road, Woods Hole, MA 02543, USA
[b] University of North Carolina, Wilmington, Center for Marine Science, 5600 Marvin Moss Lane, Wilmington, NC 28409, USA
[c] Florida State University Coastal and Marine Lab, 3618 Coastal Highway 98, St Teresa, FL 32358, USA

ARTICLE INFO

Available online 25 September 2013

Keywords:
Multibeam bathymetry
Shelf-break
CHIRP
Sea-level
Baltimore Canyon
Wilmington Canyon
Washington Canyon
Norfolk Canyon
Turbidity flow

ABSTRACT

Shelf-sourced submarine canyons are common features of continental margins and are fundamental to deep-sea sedimentary systems. Despite their geomorphic and geologic significance, relatively few passive margin shelf-breaching canyons worldwide have been mapped using modern geophysical methods. Between 2007 and 2012 a series of geophysical surveys was conducted across four major canyons of the US Mid-Atlantic margin: Wilmington, Baltimore, Washington, and Norfolk canyons. More than 5700 km^2 of high-resolution multibeam bathymetry and 890 line-km of sub-bottom CHIRP profiles were collected along the outer shelf and uppermost slope (depths of 80-1200 m). The data allowed us to compare and contrast the fine-scale morphology of each canyon system. The canyons have marked differences in the morphology and orientation of canyon heads, steepness and density of sidewall gullies, and the character of the continental shelf surrounding canyon rims. Down-canyon axial profiles for Washington, Baltimore and Wilmington canyons have linear shapes, and each canyon thalweg exhibits morphological evidence for recent, relatively small-scale sediment transport. For example, Washington Canyon displays extremely steep wall gradients and contains ~100 m wide, 5–10 m deep, v-shaped incisions down the canyon axis, suggesting modern or recent sediment transport. In contrast, the convex axial thalweg profile, the absence of thalweg incision, and evidence for sediment infilling at the canyon head, suggest that depositional processes strongly influence Norfolk Canyon during the current sea-level high-stand. The north walls of Wilmington, Washington and Norfolk canyons are steeper than the south walls due to differential erosion, though the underlying cause for this asymmetry is not clear. Furthermore, we speculate that most of the geomorphic features observed within the canyons (e.g., terraces, tributary canyons, gullies, and hanging valleys) were formed during the Pleistocene, and show only subtle modification by Holocene processes active during the present sea-level high-stand.

© 2013 Elsevier Ltd. All rights reserved.

1. Introduction

The U.S. Atlantic continental margin is one of the most extensively studied passive margins in the world. High-resolution geophysical surveys conducted by federal and state government agencies and academic institutions have generated unprecedented views of the seafloor morphology across the outer continental shelf, slope and rise between Cape Hatteras and Georges Bank (Andrews et al., 2013; Brothers et al., 2013a, 2013b; Chaytor et al., 2009; Twichell et al., 2009). Select surveys were aimed at filling gaps in data coverage and at examining the fine-scale relationships between form and process within a series of major submarine canyons. Submarine canyons on passive margins are primarily the result of erosion induced by sediment flows, but other forces such as tidal currents, internal and storm waves, submarine landslides, and biological reworking, also play important roles in canyon formation (Cacchione et al., 2002; Canals et al., 2006; Palanques et al., 2005; Paull et al., 2003, 2011; Shepard, 1981; Twichell et al., 1985; Xu et al., 2004). One goal of submarine canyon research is to better understand the relative influence of these processes in canyon development.

The shelf-edge represents a major physiographic boundary that separates fundamentally different oceanographic and sedimentary regimes (Stanley and Moore, 1983). Submarine canyons can be split into two broad categories based on their relationship to the shelf-edge: shelf-sourced and slope-sourced canyons. Shelf-sourced

* Corresponding author. Current address: Department of Oceanography and Coastal Sciences, Louisiana State University, 2151 Energy, Coast and Environment Building, Baton Rouge, LA 70803, USA. Tel.: +1 484 547 9143.
E-mail address: jobelc1@lsu.edu (J. Obelcz).

0967-0645/$ - see front matter © 2013 Elsevier Ltd. All rights reserved.
http://dx.doi.org/10.1016/j.dsr2.2013.09.013

canyons, also called "shelf-breaching" canyons (Farre et al., 1983), can extend several kilometers landward of the shelf-break. Slope-sourced canyons tend to be closely spaced (1–2 km separation), have heads located deeper than the classically defined shelf-edge (Kennett, 1982) and primarily capture sediment released during local slope failures (Brothers et al., 2013b; Pratson et al., 1994; Twichell and Roberts, 1982). During Pleistocene sea-level low-stands rivers delivered significant volumes of sediment to the outer shelf, much of which was transported directly into shelf-sourced canyons and funneled offshore to deep sea fans (Poag, 1992; Shepard, 1981). During sea-level high-stands many shelf-sourced canyons remain inactive due to being disconnected from fluvial sources (Covault and Graham, 2010; Palanques et al., 2009; Paull et al., 2011; Puig et al., 2003; Sanford et al., 1990; Shepard, 1981) but some remain active, particularly those on active margins with narrow shelves. Shelf-sourced canyons are long-lived features that continuously influence the physical and biological processes near the shelf-edge; however, the sources of sediment and down-canyon transport mechanisms during high-stand conditions remain poorly understood.

The U.S. Atlantic margin contains between 30 and 40 shelf-sourced submarine canyons (Andrews et al., 2013). Hudson Canyon, to the east of New Jersey, is perhaps the most widely recognized due to its significant relief (> 1000 m at the shelf-edge), prominent shelf-valley and well-developed deep sea channel that extends hundreds of km seaward of the continental slope (Butman et al., 2006). This paper is focused on four major, shelf-sourced canyons located to the south of Hudson Canyon (from north to south): Wilmington, Baltimore, Washington, and Norfolk canyons (Fig. 1). Our analysis of new high-resolution bathymetric and sub-bottom data provides a new approach to delineating some of the physical boundary conditions that govern the sedimentary, oceanographic and biologic processes operating in and around shelf-sourced canyons. Using these data, we aim to answer the following questions: (1) what are the first-order morphological differences between the four canyons? (2) What are the potential linkages between fine-scale canyon morphology and sedimentary and oceanographic processes? and (3) What is the magnitude and relative importance of modern sedimentary processes in canyon formation?

2. Background

Although the formative relationship between slope-sourced and shelf-sourced submarine canyons remains uncertain, both types of canyons are influenced by changes in base level (sea-level fluctuations) and sediment flux at the shelf-edge. The "headward erosion" hypothesis proposed by Farre et al. (1983) states that "young" slope-confined canyons propagate up-slope via local mass failure, capturing smaller canyons and rills along the way, until the shelf itself is breached, becoming a "mature", shelf-sourced canyon. Once breaching the shelf, canyons are more likely to capture river systems that cross the continental shelf during sea-level low-stands, in addition to becoming a conduit for sediment that is not terrestrially sourced (such as sediment entrained in along-shore currents) (Farre et al., 1983; lo Iacono et al., 2011; Twichell et al., 1977). During periods of sea-level low-stand, rivers discharge sediment near the shelf-edge and the locus of deposition shifts to deeper waters of the slope and rise (Catuneanu, 2006; Piper and Normark, 2001; Posamentier and Vail, 1988). Rivers discharging sediment-laden water directly into shelf-sourced canyon heads may generate hyperpycnal flows (Mulder and Syvitski, 1995) that bypass and erode the upper reaches of canyons, leading to further landward entrenchment (Farre et al., 1983). During sea-level high-stands, shelf depocenters shift landward and most sediment becomes trapped in coastal estuaries and embayments, particularly along passive margins with wide continental shelves (Catuneanu, 2006; Posamentier and Vail, 1988). Along the U.S. Atlantic margin, sediment delivery to the shelf-edge during sea-level high-stands is reduced dramatically and many canyons become sites of enhanced hemipelagic sediment accumulation (Mountain et al., 2007; Sanford et al., 1990).

During sea-level high-stands, the primary sediment transport mechanisms into shelf-sourced canyons include the following: (1) storm induced transport of relict shelf sand and silt (Stanley et al., 1986; Xu et al., 2010); (2) transport of fine grained sediment

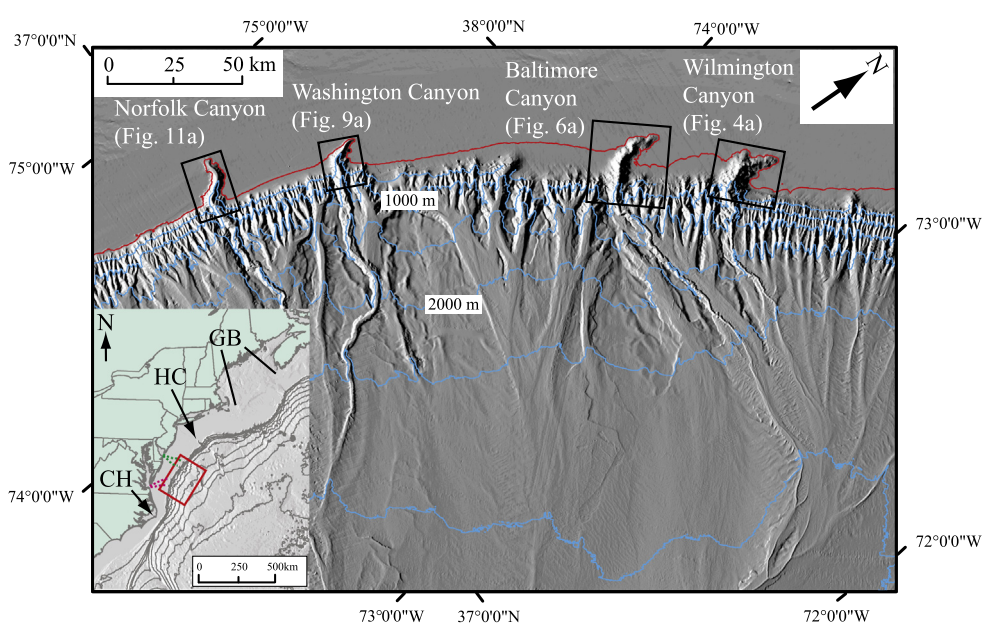

Fig. 1. Shaded relief map of study area. Illumination angle is 315° (this applies to all hillshades presented in this paper).The red contour represents the 120 m isobath, and blue contours represent 500 m isobaths. *Lower left inset*: Red box is extent of relief map. Contours are every 500 m. Abbreviations: CH: Cape Hatteras; GB: Georges Bank; HC: Hudson Canyon. Dashed green lines are paths of paleo-Delaware River and dashed purple lines are paths of paleo-Susquehanna River. (For interpretation of the references to color in this figure legend, the reader is referred to the web version of this article.)

by tidal currents, density currents and internal waves (Cacchione et al., 2002; Gardner, 1989b; Micallef and Mountjoy, 2011; Shepard et al., 1979); (3) debris flows down canyon walls, partially in response to sediment spillover off the shelf (Paull et al., 2011; Sanford et al., 1990; Xu et al., 2010).

Previous studies of Wilmington, Baltimore, Washington and Norfolk canyons collected low-resolution geophysical data (e.g., singlebeam echosounders, early-generation multibeam, mid-range sidescan sonar and seismic reflection profiles), sediment cores, current-meter measurements and observations from submersible dives (Farre et al., 1983; Forde et al., 1981; Gardner, 1989a,b; Kelling and Stanley, 1970; McGregor et al., 1979; Sanford et al., 1990; Stubblefield et al., 1982). From the observed deep-sea channel-levee systems and fan development at abyssal depths, it is clear that these canyons funneled large amounts of sediment across the slope and rise during the Pleistocene (Forde et al., 1981; Poag, 1992; Twichell et al., 1977). A number of sedimentary processes appear to be active in mid-Atlantic submarine canyons, including transport of shelf sediments over the canyon rims and down steep gullies to the canyon floor (Sanford et al., 1990). Coarse to medium grained, shelly terrigenous sands are observed adjacent to the canyon heads, but transport of this coarse sediment into canyons during the Holocene most likely occurs episodically during major storms (Forde et al., 1981). In general, surficial sediment shows a decrease in grain size from the canyon head towards the slope, suggesting that currents winnow the fine-grained material (Farre et al., 1983; Kelling and Stanley, 1970; Stanley et al., 1986). Localized slumps, slides and debris aprons are observed along the base of steep sidewalls; in many cases, destabilization due to bioerosion appears to play an important role in localized collapse of canyon walls (Farre et al., 1983; Forde et al., 1981; McGregor et al., 1979; Stanley, 1974; Stubblefield et al., 1982).

3. Methods

Multibeam bathymetry data and CHIRP sub-bottom profiles were acquired during three geophysical cruises. In June 2011, more than 5700 km^2 of multibeam bathymetry data were collected in Baltimore, Washington and Norfolk canyons aboard the NOAA Ship *Nancy Foster* using a hull-mounted Kongsberg Simrad EM1002. In July–August 2007, the NOAA Ship *Thomas Jefferson* collected multibeam bathymetry in the head and adjacent shelf areas of Norfolk Canyon also using a Kongsberg Simrad EM-1002 (Rod Mather, 2011, Pers. comm.). In September 2011, the NOAA Ship *Okeanos Explorer* surveyed Wilmington Canyon using a Kongsberg Simrad 302. Bathymetry data were edited, processed and gridded using Caris HIPS/SIPS to 10-m resolution for the *Nancy Foster* and *Thomas Jefferson* data and 25-m for the *Okeanos Explorer* data. All of the multibeam bathymetry presented in this paper (except the *Thomas Jefferson* data) is available in a USGS open-file report (Andrews et al., 2013). Interpretations for bathymetric data were conducted using ESRI ArcGIS v. 9.3.

In May 2012 the USGS conducted geophysical surveys aboard the M/V *Tiki XIV* using an Edgetech 512i sub-bottom profiler (emitting a 0.5–4.5 kHz swept-frequency signal) and a differential GPS system for navigation fixes. Surveys in Baltimore, Washington and Norfolk canyons yielded a total of ~890 line-km, but sub-bottom penetration was severely limited in and around Washington Canyon. Sub-bottom data were processed (swell filtering, selective muting of water column, and time varying gains) using the *SIOSEIS* software package. All seismic reflection profiles were then plotted and interpreted using the *Kingdom Suite* software package.

4. Geomorphic observations

Basic morphometric parameters were computed from each canyon system to examine their differences and similarities (Table 1), including maps of the seafloor gradient (Fig. 2) and canyon thalweg profiles (Fig. 3). Below we summarize geomorphic observations of each canyon starting with (i) first-order descriptions of canyon shape, symmetry, character of the sidewalls and of the thalweg profile; then (ii) detailed descriptions of canyon head and canyon rim morphologies, including steps, platforms, channels, troughs and bedforms; and finally (iii) descriptions of fine-scale morphological features within the canyons and their tributaries. Note canyon sidewalls are referenced as "northern" and "southern" despite meanders and variation in axial trend.

4.1. Wilmington Canyon

Wilmington Canyon (WiC) is located ~130 km southeast of Delaware Bay and extends approximately 19 km landward of the shelf-edge (Farre et al., 1983; Kelling and Stanley, 1970; Sanford et al., 1990; Fig. 1). WiC is the largest of the four canyons in terms of length, width and depth (Table 1). Its axial trend is dominated by a large, ~45° eastward bend about halfway along its length within the shelf (Fig. 4A), but several shorter-wavelength meanders are also observed. Seaward of the axial bend, the density of tributary canyons and gullies increases dramatically, and the variation in axial gradient also increases (Fig. 3). Canyon cross-sections are mostly U-shaped headward of the axial bend and V-shaped seaward of the bend (Fig. 4B). Subtle and intermittent 50–100 m wide, 5 m deep thalweg incisions are observed along the length of the canyon (red lines in Figs. 4A and

Table 1
Basic geomorphic parameters of the four canyons: "distance into shelf" is the distance the canyon is incised landward of the shelf-edge; "mean down-axis canyon gradient" is the average gradient of the axial thalweg from the canyon head to the shelf-edge (dashed black line, Figs. 2A, 3A, 4A, and 5A); "first axial bend" is the distance from the canyon head to the first major axial meander (measured along the canyon axis); "number of v-incisions" and "length of v-incisions" are counts of sections showing evidence for axial incision and length of incisions, respectively; "thalweg sinuosity (S)" is calculated by dividing the canyon axis into 10-km segments, where S=(length of segment measured along thalweg/shortest distance from beginning to end of segment). The S values of all segments of the canyon axis are then averaged, giving S; finally, "width of the canyon floor" lists the approximate minimum and maximum widths of the canyon floor (measured between side-walls).

	Wilmington	Baltimore	Washington	Norfolk
Distance into shelf (km)	19	15	10.5	16.5
Depth at shelf-edge (m)	1160	700	700	800
Width at shelf-edge (km)	11	8.5	6	8
Depth at canyon head (m)	80	100	100	80
Mean down-axis gradient (deg.)	2.9	2.1	3.2	2.7
First axial bend (km)	13	5	10	7.5
Number of v-incisions	5	6	2	1
Length of v-incisions (km)	< 1	< 1	4	< 0.5
Distribution of v-incisions	Entire axis	Canyon head/first bend	Entire axis	First bend
Width of canyon floor (m)	200–1200	300–750	300–850	250–1000
Thalweg sinuosity (S)	1.09	1.19	1.05	1.07

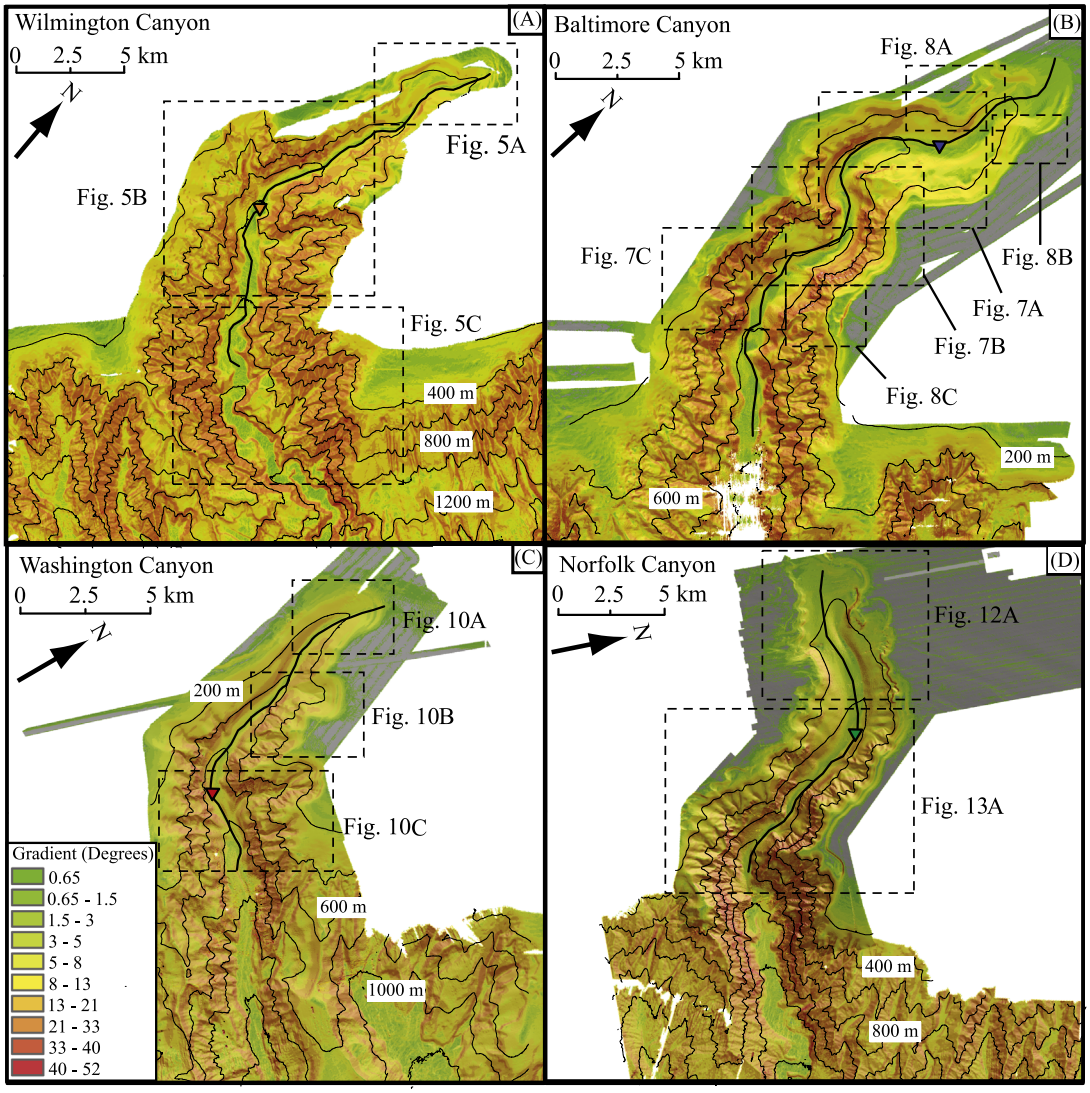

Fig. 2. Entire extent of all canyons studied, shaded based on gradient (green: flat, red: steep). Thin black lines are 200 m contours, thick black lines are extent of axial profiles shown in Fig. 3, and inverted triangles are approximate locations of first axial bends. (For interpretation of the references to color in this figure legend, the reader is referred to the web version of this article.)

5). Overall, the northern wall is locally steeper and contains a greater number of tributary canyons than the southern wall (Figs. 2A and 4A), particularly seaward of the axial bend.

The headward section of WiC is characterized by a local meander in the canyon rim and four to five 100–200 m-wide bathymetric undulations near the canyon head that trend perpendicular to the canyon axis (Fig. 5A). Farther down-canyon, the ~45° axial bend coincides with the confluence of a tributary canyon that indents the southern wall; the thalweg profile of the tributary canyon shows a subtle change in gradient as it merges with the main axis of the canyon (Fig. 5B). Seaward of the bend, both walls of WiC are cut by a series of steep (typically > 6° along axis) tributary canyons with dendritic plan-view morphology and heads located just below the regional canyon rim. Here, the confluences of tributary canyons with the main axis coincide with 20–150 m-high bathymetric escarpments that resemble hanging valleys (Fig. 5C). The walls of tributary canyons are characterized by steep, narrow gullies, some of which also exhibit hanging valleys at their confluences with tributary canyons (e.g., Fig. 5B). Seaward of the axial bend, WiC's sidewalls adjacent to the canyon axis contain pervasive evidence for mass wasting, including landslide scarps and scalloped slopes (Fig. 5C).

4.2. Baltimore Canyon

Baltimore Canyon (BC) is located ~30 km to the south of WiC and is smaller in all dimensions (Fig. 1 and Table 1). The axis of BC has several broad (~5 km wavelength) meanders starting ~5 km down canyon (Fig. 6A). BC is more U-shaped and/or flat-bottomed relative to WiC (Fig. 6B). Narrow thalweg incisions are observed only along the landward 10 km (300–600 mbsl) of the canyon axis (Figs. 6A and 7A). BC's axial profile has the lowest mean gradient of the four canyons (Table 1); its axial gradient becomes highly variable ~8 km from the canyon head (Fig. 3B). Although the steepness and roughness between the northern and southern walls is relatively symmetric over the length of the canyon (Figs. 2B and 6B), both walls show increased roughness starting ~8 km down canyon, including several near-vertical escarpments part-way down the canyon wall (Fig. 7B). Overall, gully thalwegs and inter-gully ridges are shorter and less angular than those of WiC.

The headward stretch of BC contains a series of bathymetric steps and terraces just below the canyon rim in depths of 110–130 m below sea-level (mbsl) that can be traced laterally for several kilometers, following the curvature of the canyon rim

(Figs. 7 and 8). Some of the terraces coincide with stratigraphic horizons imaged in sub-bottom profiles (Fig. 8A); others do not (Fig. 8B). At a distance of 13 km down-canyon, a step along the southern rim is disrupted by a set of unusual crescentic troughs that are ~2 km long and 10 m deep (Fig. 7C). The troughs have the surficial expression of back-tilted slump blocks, or perhaps fluid expulsion features (Hill et al., 2004). Unfortunately, sub-bottom penetration was very limited and internal stratigraphy of these features was not imaged. Below the troughs, sidewall gullies debouche onto platforms located ~100–200 m above the canyon floor. A small channel visible in bathymetric profiles intersects the southern canyon rim above a broad, undulating bathymetric platform (Fig. 8C).

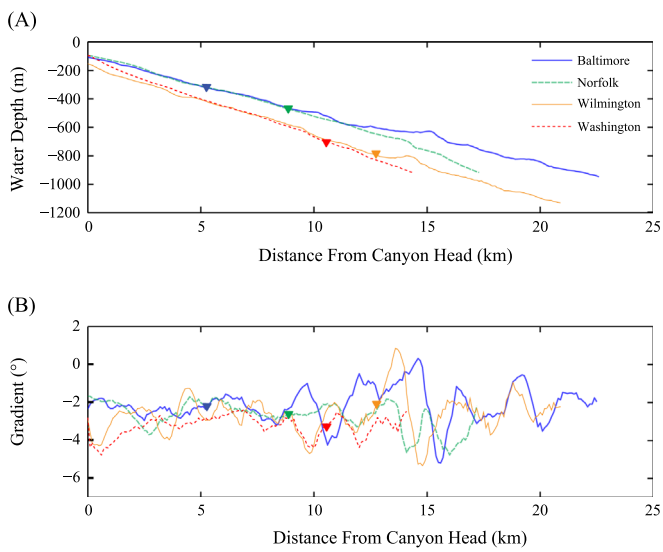

Fig. 3. (A) Canyon thalweg profiles plotted together. Profiles were measured from the canyon head to the regional shelf-edge. (B) Gradient variation along axial profiles. A 900 m smoothing window was applied to minimize short-wavelength variation. Inverted triangles represent approximate location of first down-axis canyon meander.

4.3. Washington Canyon

Washington Canyon (WC) is located ~130 km east of Chesapeake Bay (Fig. 1) and is the smallest of the four canyons surveyed (Table 1). The axis of WC changes orientation approximately 10 km from the canyon head (Figs. 2C and 9A), then trends perpendicular to the shelf-edge for the remaining 6 km out to the shelf-edge. WC has the steepest mean axial gradient of the four canyons (Table 1); it has a relatively smooth axial gradient headward of the bend, and increased variability seaward of the bend (Fig. 3B). Of the four canyons, WC contains the most distinctive evidence for thalweg incision along its length (red lines in Figs. 9A and 10C). The axial incisions begin 5 km from the canyon head and are nearly continuous out to the shelf-edge. Seaward of WC's bend, the canyon contains a higher density of steep tributary canyons and gullies (Figs. 2C and 9A), particularly along the northern wall, which has greater roughness and local steepness than the southern wall.

Several bathymetric steps are observed throughout the canyon, including an angular step along the southern wall that can be traced for ~4 km seaward of the canyon head (Fig. 9A) and a series of rounded, ~100 m-wide steps below the head of the main canyon (Fig. 10A) and a tributary canyon (Fig. 10B). A series of short-wavelength (~40 m), 1.0–1.5 m-high sediment waves are visible on the shelf above the canyon head (Fig. 10A) and adjacent to the northern rim above a tributary canyon (Fig. 10B); the wave-fields are wedge-shaped in plan-view, widening towards the canyon rim. The northern canyon wall, between the thalweg and the ~500 m isobath, is steeper and contains greater

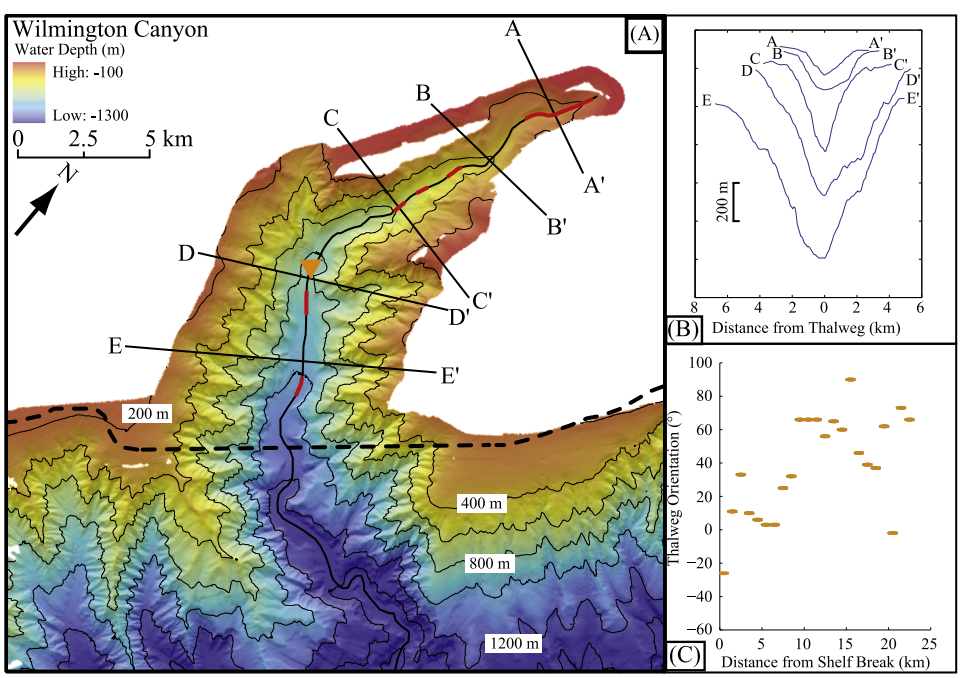

Fig. 4. (A) High-resolution (25 m cell size) shaded relief of Wilmington Canyon. Features of note: canyon thalweg (solid black line), canyon floor v-incision (red lines on canyon thalweg) cross-sectional profiles (black lettered lines), 200 m isobaths (thin black lines), first major axial bend (inverted triangle), and regional shelf-edge (dashed black line). Bathymetry for cross-sectional profiles in (B), Figs. 6B, 9B, and 11B was derived from the NOAA Coastal Relief Model (CRM) where our bathymetry was absent. (B) Profile views of cross-sections. (C) Axial orientation versus distance from the shelf-edge. The canyon axis was split into 1-km segments and the orientation of each segment was measured relative to a landward-pointing vector perpendicular to the shelf-edge (e.g., 0° is perpendicular to the regional trend of the shelf-edge; clockwise = positive, counterclockwise = negative). (For interpretation of the references to color in this figure legend, the reader is referred to the web version of this article.)

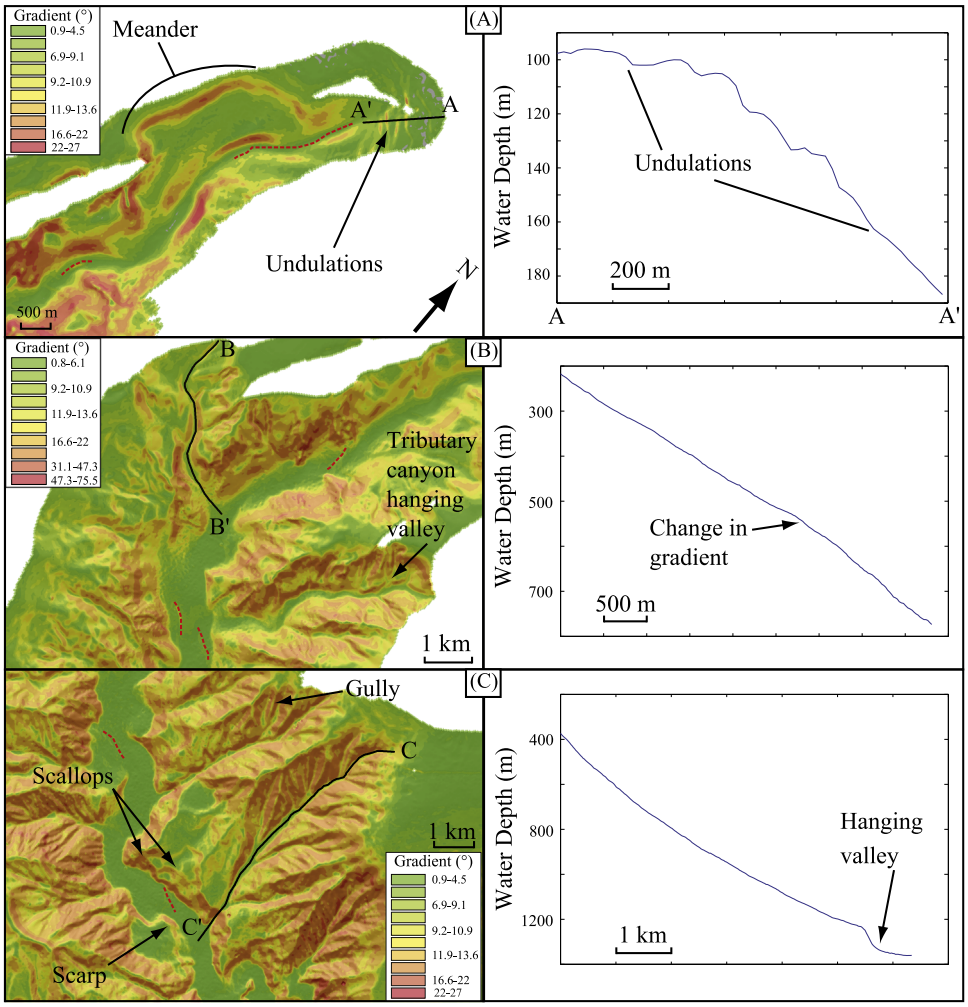

Fig. 5. Selected geomorphic features in Wilmington Canyon (WiC): (A) Meander at the head of WiC; A–A′ is a cross-sectional profile of the undulations that feed into WiC's head. Red dashed lines are areas of axial incision. (B) WiC's main axial bend and several tributary canyons. B–B′ is a cross-sectional profile of a major tributary canyon. (C) Several of WiC's down-axis tributary canyons. C–C′ is a cross-sectional profile of a tributary canyon with a prominent hanging valley. (For interpretation of the references to color in this figure legend, the reader is referred to the web version of this article.)

geomorphic evidence for mass wasting than the southern wall (Fig. 10C). In general, hanging valleys are not observed at the confluences between tributary canyons and the main canyon axis (e.g., C–C′ in Fig. 10C).

4.4. Norfolk Canyon

Norfolk Canyon (NC), located 45 km south of WC, has a sigmoidal shape in plan-view (Figs. 2D and 11A). Like the other canyons, a broad axial bend ~9–10 km seaward of its head coincides with a change from relatively smooth gradients along the headward section of the thalweg profile to highly variable gradients along the seaward section (Fig. 3). The mean axial profile gradient is 2.7° (Table 1). Only a short section of the canyon axis ~400 mbsl contains bathymetric evidence for thalweg incision (Fig. 11A). Just seaward of the bend, the canyon sidewalls become highly dissected by tributary canyons and gullies (Fig. 11A). Throughout the canyon the northern wall is steeper and has a rougher appearance than the southern wall (Figs. 2D and 11B).

The canyon rim morphology and sub-bottom stratigraphy observed along NC are more distinctive than the other canyons (Fig. 12A). Sub-bottom data near the canyon head show stratigraphic beds beneath the adjacent shelf that are truncated by steep escarpments (Fig. 12B). A series of embayments surrounding the canyon head appear to be surficial expressions of buried shelf channels that merge with the main axis of the canyon (Fig. 12A). The floors of the buried channels are filled with a chaotically, relatively high-amplitude package, and above this is a horizontally bedded, lower amplitude package. Strata imaged in sub-bottom profiles also show evidence for repeated cut and fill episodes (Figs. 12B and C).

A series of nearly continuous bathymetric steps just below the canyon rim can be traced to the shelf-edge along the northern rim (Fig. 13A). Near the shelf-edge, a broad terrace on the north wall appears to correlate with a stratigraphic horizon observed in sub-bottom profiles (red dashed line, A–A′, Fig. 13B). The morphology of the southern rim is highly irregular, showing short escarpments and steep indentations (Fig. 13A); however, data coverage is limited towards the shelf-edge. NC's axis has minimal surficial expression of incision, but evidence of previous incision is apparent on seismic reflection profiles (Fig. 13C).

4.5. Bathymetric steps below the canyon rim

As highlighted above, BC, WC and NC each contain bathymetric steps (or terraces) located at or below their canyon rims. Plots of terrace depth versus absolute distance from the shelf-edge reveal several trends (Fig. 14). For example, terrace depths in BC range

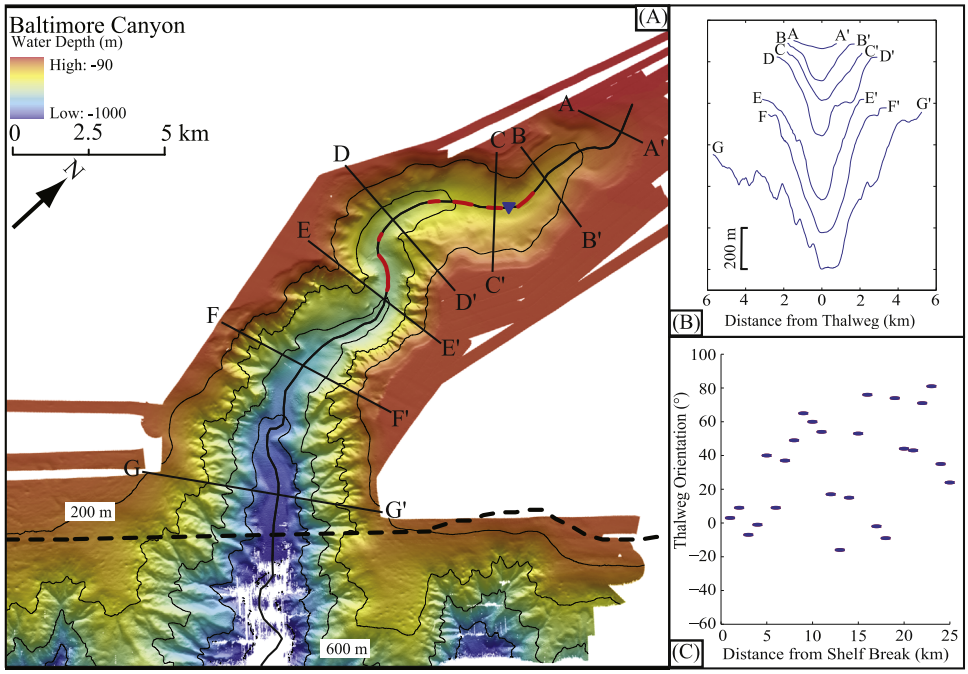

Fig. 6. (A) High-resolution (10 m cell size) shaded relief of Baltimore Canyon. Features of note: canyon thalweg (solid black line), canyon floor incision (red lines on canyon thalweg), cross-sectional profiles (black lettered lines), 200 m isobaths (thin black lines), first major axial bend (inverted triangle), and regional shelf-edge (dashed black line). (B) Profile views of cross-sections. (C) Axial orientation versus distance from the shelf-edge (see Fig. 4 caption for explanation). (For interpretation of the references to color in this figure legend, the reader is referred to the web version of this article.)

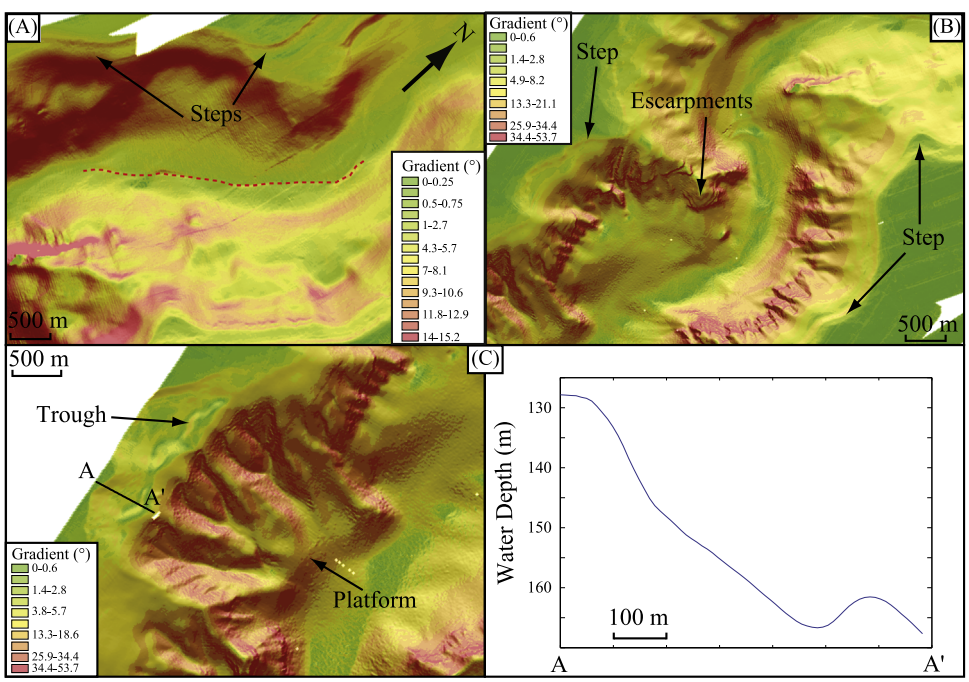

Fig. 7. Selected geomorphic features in Baltimore Canyon (BC): (A) Canyon floor v-incisions (red dashed line). (B) BC's meandering canyon axis. (C) "Trough" features on BC's south wall; A–A′ is a cross-sectional profile of one of these features. (For interpretation of the references to color in this figure legend, the reader is referred to the web version of this article.)

from 115 to 165 mbsl and can be separated into two groupings. The first grouping shows terrace depths becoming shallower in a landward direction; the second shows variable depths about a median value of 128 mbsl (Figs. 8A, B and 14A). Terraces of the second grouping are observed ~2 km seaward of the canyon head to ~10 km headward of the shelf-edge. WC's terraces have no obvious depth trend (Fig. 14B). The majority of depths fall between 140 and 110 mbsl, with three points ~11 km landward of the shelf-edge with depths of ~85 mbsl. NC also shows two groupings of terrace depths (Fig. 14C): from 2 to 5 km headward of the shelf-edge, terraces become shallower towards the canyon head (from 145 mbsl to 120 mbsl, Fig. 13B); the remaining 10 km headward of the shelf-edge, terrace depths range from 125 to 105 mbsl and have a mean depth of ~115 mbsl.

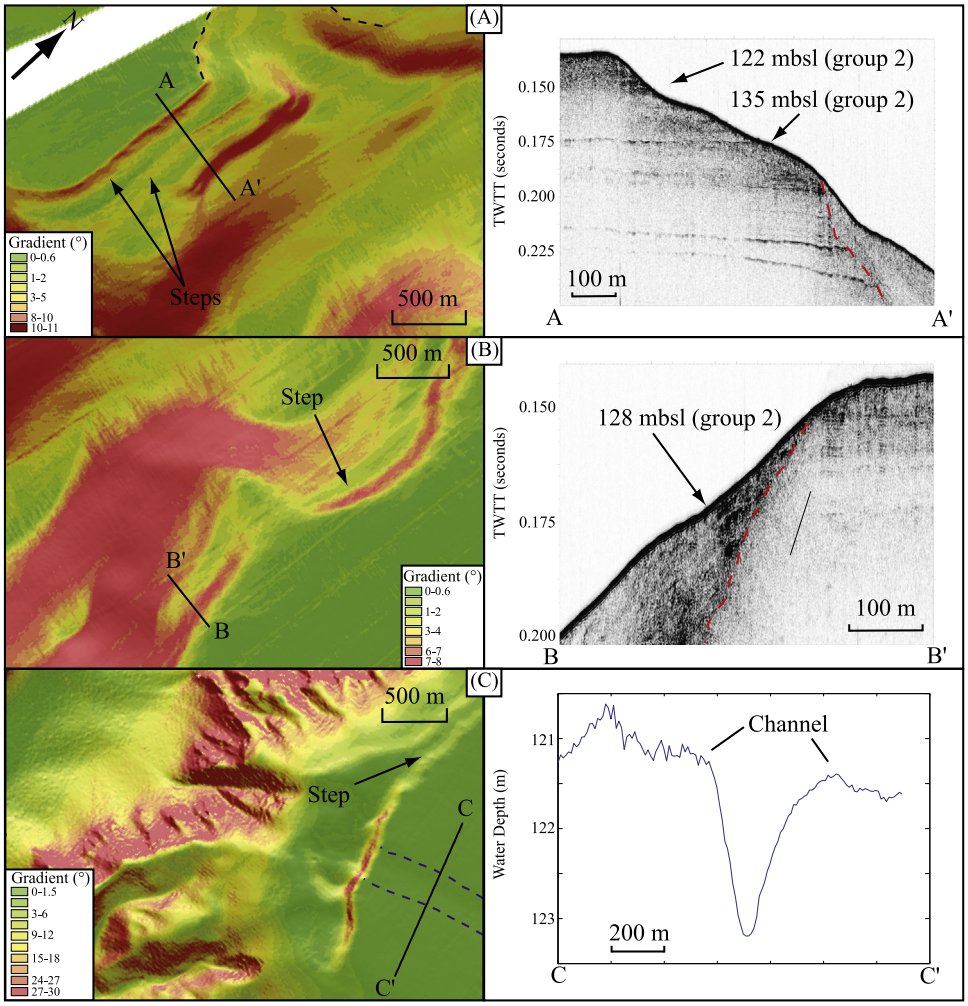

Fig. 8. Selected geomorphic features in Baltimore Canyon (BC): (A) steps and embayment (black dashed line) in southern BC head. A–A′ and B–B′ are CHIRP profiles. Red dashed line in the CHIRP profile indicates base of canyon head infill in A–A′ and B–B′. (B) Steps in north BC head. (c) BC north wall "platform". C–C′ is a cross-sectional view of a small channel (blue dashed line). (For interpretation of the references to color in this figure legend, the reader is referred to the web version of this article.)

5. Discussion

5.1. Fluvial influence on canyon shape

Shelf-sourced submarine canyons along passive margins are generally most active during periods of lowered sea-level when sediment supply to the canyons is greatest (Catuneanu, 2006). A seaward shift in shoreline position allows canyons to capture sediment directly from fluvial and littoral systems of the continental shelf. During Late-Pleistocene sea-level low-stands, each of the four Mid-Atlantic canyons was probably connected to fluvial drainage systems (Forde, 1981; Kelling and Stanley, 1970; Twichell et al., 1977). During the last glacial maximum (LGM) when eustatic sea-level was ~120 m lower than today (Peltier and Fairbanks, 2006), the shoreline may have intersected the canyons on either side of the major axial bends (red contour in Fig. 1). The canyon reaches that extend landward of the 120 m isobaths probably experienced greater fluvial influence than the reaches farther offshore. Kelling and Stanley (1970) proposed that WiC and BC were shaped by the same fluvial system, based on their proximity, similar sizes, and stratigraphic architecture. Pratson et al. (1994) speculated that southward-trending currents deflected the Hudson River outflow to the south, possibly linking it with WiC. Knebel and Spiker (1977) attributed cut-and-fill stratigraphy northeast of WiC to a meandering fluvial system, but proposed the former Great Egg and/or Delaware rivers as potential sources. It is possible that the bidirectional orientation of WiC (Fig. 4A) is related to paleodrainages from the west (Delaware) and the northwest (Hudson). Furthermore, if WiC had two major fluvial sources (either concurrently or at different times), it could explain why it is larger in all dimensions than the other canyons.

A sharp contrast in sediment mineralogy on the shelf (Kelling et al., 1975) suggests that the two southern canyons (WC and NC) had different sources of sediment than the two northern canyons (BC and WiC). WC and NC have also been linked to common fluvial sources (Forde, 1981), such as the Susquehanna River-Chesapeake Bay drainage system (Colman et al., 1990; Forde, 1981), though this paleo-shelf channel is poorly established (Knebel and Spiker, 1977). NC also displays evidence for two different fluvial sources (or a delta system with multiple distributary channels) modifying it: the canyon head is oriented E–W, but CHIRP sub-bottom profiles (e.g., Fig. 12) show buried channels that entered the canyon from the northwest. NC's larger size and complex orientation in relation to WC may be the product of a greater magnitude of fluvial influence.

The differing sinuosity, *S*, of the four canyons (Table 1) may also be a product of low-stand fluvial influence. BC contains the greatest sinuosity and the lowest average thalweg gradient, whereas WC contains the lowest sinuosity and the greatest average gradient. Based on fluvial analogs, these patterns may indicate differences in

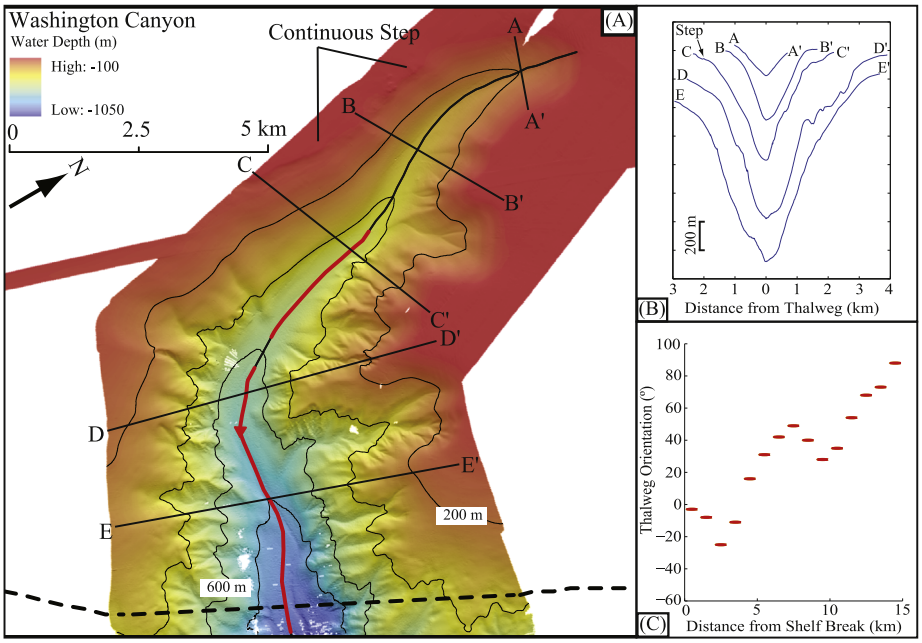

Fig. 9. (A) High-resolution (10 m cell size) shaded relief of Washington Canyon (see Fig. 1 for regional location). Features of note: canyon thalweg (solid black line), canyon floor incision (red lines on canyon thalweg) cross-sectional profiles (black lettered lines), 200 m isobaths (thin black lines), first major axial bend (inverted triangle) and regional shelf-edge (dashed black line). (B) Profile views of cross-sections. (C) Axial orientation versus distance from the shelf-edge (see Fig. 4 caption for explanation). (For interpretation of the references to color in this figure legend, the reader is referred to the web version of this article.)

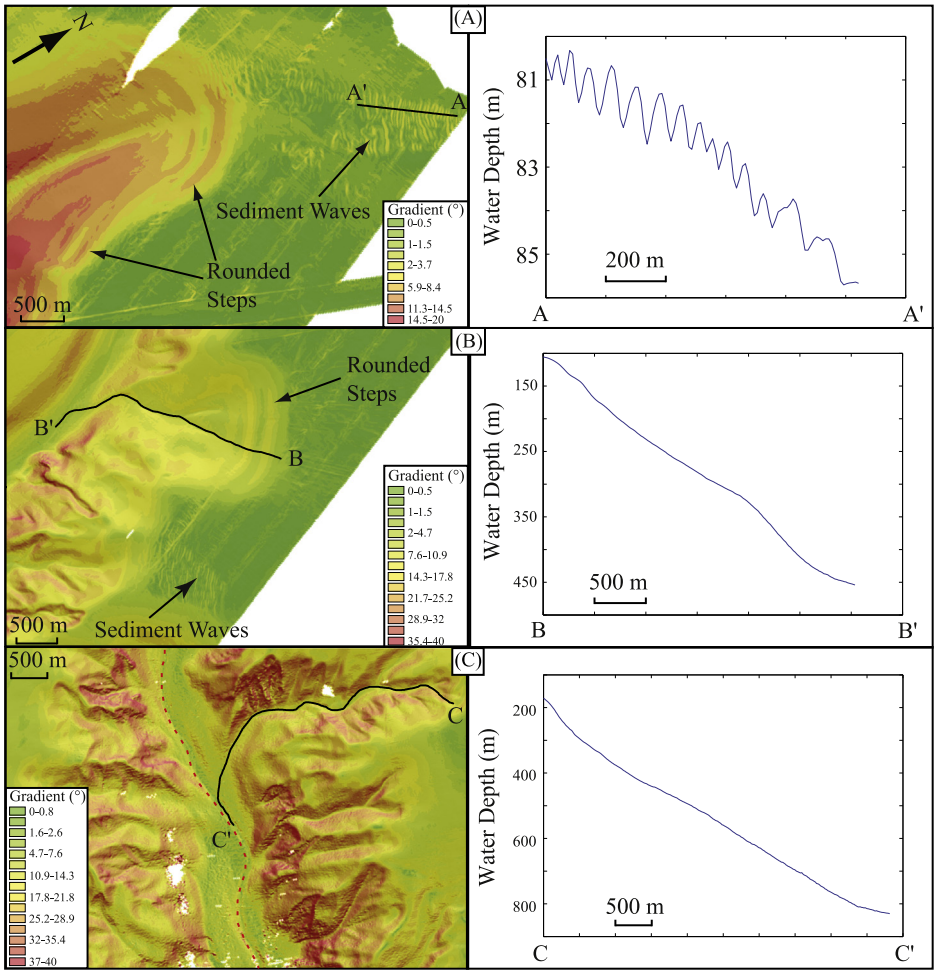

Fig. 10. Select geomorphic features in Washington Canyon (WC): (A) sediment waves feeding into the head of WC. A–A′ is a cross-sectional profile of the sand waves. (B) WC's headward north wall. B–B′ is a cross-sectional profile of the axis of a small tributary canyon. (C) Examples of relatively continuous axial incision (dashed red line) and a cross-sectional profile down the axis of a tributary canyon (C–C′). (For interpretation of the references to color in this figure legend, the reader is referred to the web version of this article.)

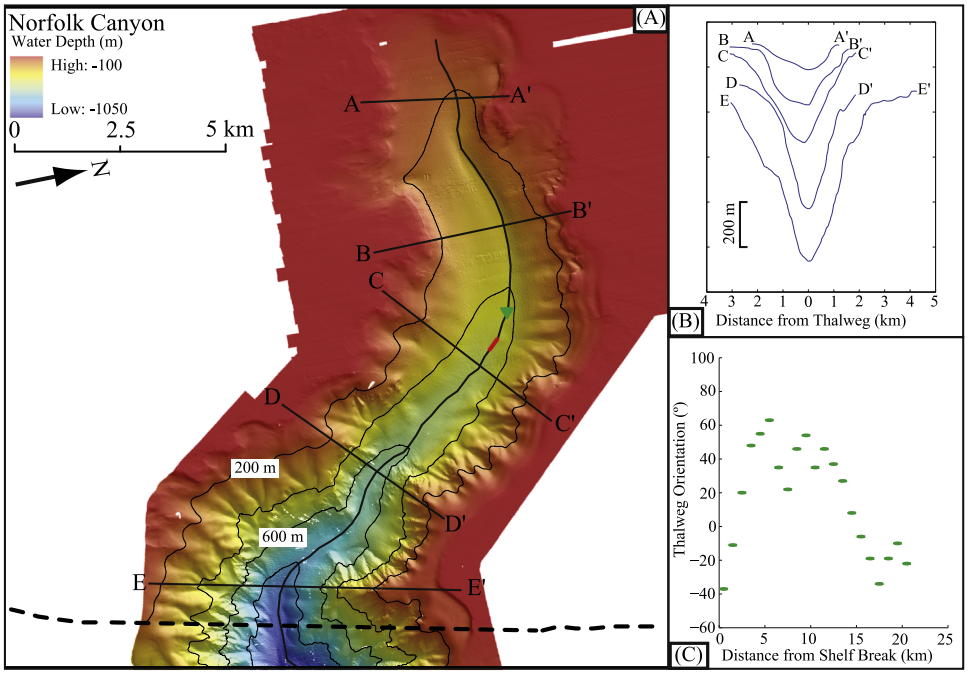

Fig. 11. (A) High-resolution (10 m cell size) shaded relief of Norfolk Canyon (see Fig. 1 for regional location). Features of note: canyon thalweg (solid black line), canyon floor incision (red lines on canyon thalweg), cross-sectional profiles (black lettered lines), 200 m isobaths (thin black lines), first major axial bend (inverted triangle), and regional shelf-edge (dashed black line). (B) Cross-sectional bathymetric profiles. (C) Axial orientation versus distance from the shelf-edge (see Fig. 4 caption for explanation). (For interpretation of the references to color in this figure legend, the reader is referred to the web version of this article.)

the frequency and/or grain size of erosive turbidity flows discharged from river mouths into the canyons during periods of lowered sea-level. For example, fluvial channels with gentle gradients and high *S* are often associated with high discharge and transport of fine-grained sediment, whereas channels with low *S* and high gradients are often linked to episodic discharge and coarse-grained sediment transport (Rosgen, 1994).

5.2. Potential influence of coastal processes on canyon shape

Canyons extending farther landward are more likely to capture fluvial and marine sediments that are transported across the shelf, regardless of sea-level position (e.g., Palanques et al., 2006; Twichell et al., 1977; Xu et al., 2010). During the LGM, the shoreline in the study region may have been only 2–6 km landward of the present-day shelf-edge (red isobath, Fig. 1). Coastal processes, including along-shore transport of sandy shelf sediment, would have dominated sediment transport along the outer shelf. Much of this sediment may have been transported over the rim of canyons and into steep tributary canyons and gullies, analogous to U.S. West Coast canyons that are presently influenced by littoral sediment input (Xu et al., 2010). The extreme steepness of local slopes seaward of the axial bends is expected to inhibit deposition and promote the generation of erosive sediment flows, which in turn may increase the roughness of the canyon walls. In contrast, headward of the axial bends the total relief and steepness of the canyon walls decreases and the morphology appears smoothed by sediment drape, sometimes asymmetrically between sidewalls. Studies of other shelf-sourced canyons, such as Palamós Canyon of the NW Mediterranean margin, document asymmetric current velocities along opposite canyon walls during major storm events (Palanques et al., 2005). Combined, these processes may help explain the asymmetric steepness and roughness between the canyon sidewalls. Storm induced resuspension and littoral transport of shelf sediments in a net southward direction (Lentz, 2008) may have generated greater frequency of erosive sediment flows down the northern sidewalls (Fig. 15).

5.3. Bathymetric steps and terraces below the canyon rim

Previous studies suggested the bathymetric steps, or terraces, observed below the canyon rims may be associated with either wave-base erosion along Late-Pleistocene paleoshorelines or preferential erosion along lithologic boundaries (Kelling et al., 1975). The terraces mapped in BC and NC decrease in depth with distance landward of the shelf-edge until they reach depths of 115–130 mbsl, at which point they level off (Fig. 14). Terraces deeper than ~130 mbsl appear to be associated with outcropping strata that have been truncated along the canyon walls (e.g., Fig. 13b; Group 1 in Fig. 14). Sub-bottom reflectors are observed to terminate at bathymetric steps along the canyon walls, and the reflectors appear to be seaward dipping, thus explaining the increasing depth of these terraces closer to the shelf-edge. Terraces mapped closer to the canyon heads tend to fluctuate about a mean depth of ~120 mbsl, the inferred position of the Late-Pleistocene Nicholls paleoshoreline (Thieler et al., 2007; Group 2 in Fig. 14). Such features have been observed in other places, such as the Danube Canyon in the Black Sea (Popescu et al., 2004), where a bathymetric step continuous for over 100 km along the margin has been attributed to a relict paleoshoreline. Although Goff et al. (2013) proposed that the Nicholls shoreline is not a continuous feature across the entire mid-Atlantic margin, it is plausible small spans of shoreline within BC and NC could have remained intact through transgression, explaining their discontinuous nature. The variation about 120 mbsl may be due to varying rates of sediment aggradation and drape on top of wave-cut surfaces associated with paleoshorelines (e.g., Figs. 7A and B).

5.4. Hanging valleys

Tributary canyons that merge with the main canyon axis at a hanging valley (i.e., hanging valleys) are most common in WiC.

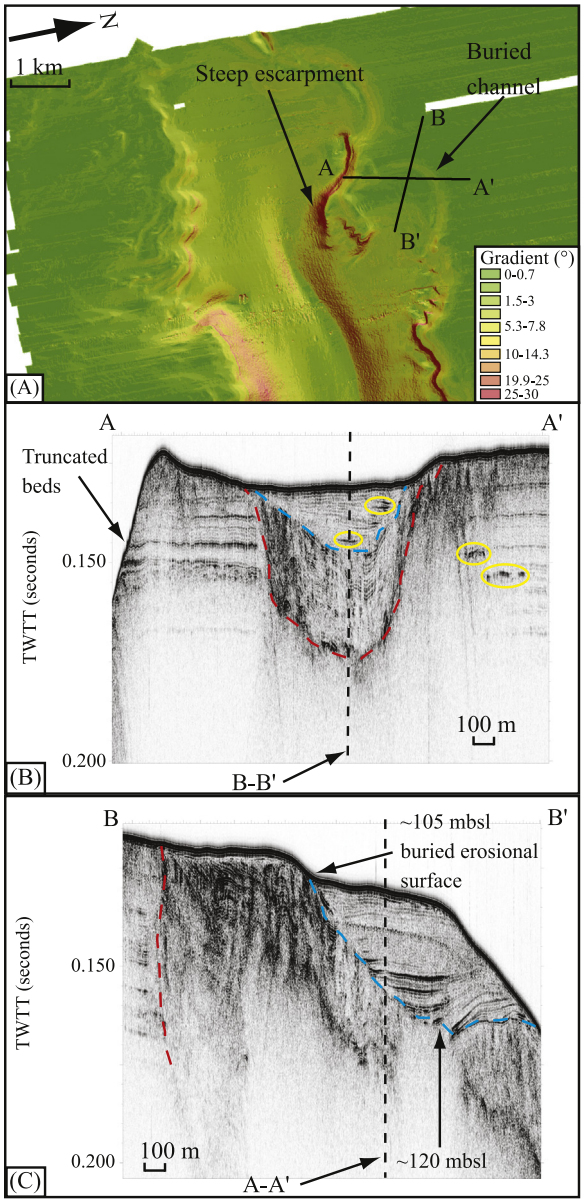

Fig. 12. Select geomorphic features in Norfolk Canyon (NC): (A) steep escarpments and buried channels in NC's head. (B) CHIRP profile across a buried channel. Red dashed line in (B) and (C) represents the base of the channel. Light blue dashed line in (B) and (C) represents a major depositional boundary; yellow circles appear to be gas-charged sediment layers; dashed black line represents intersection with CHIRP profile in (C). (C) Down-dip CHIRP profile within the same buried channel. (For interpretation of the references to color in this figure legend, the reader is referred to the web version of this article.)

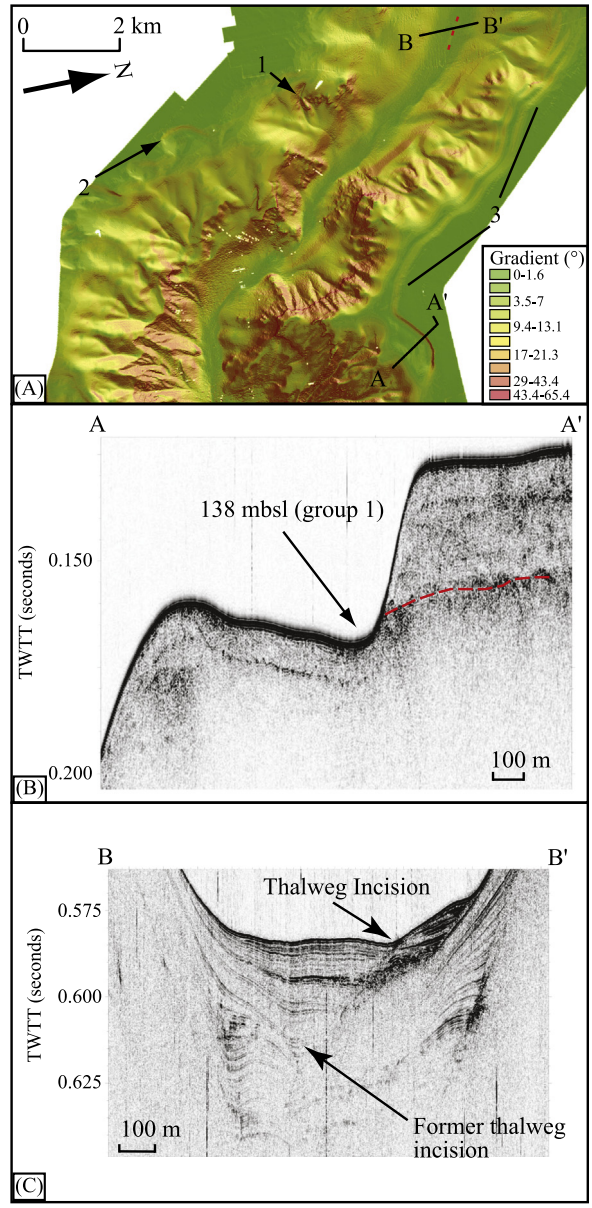

Fig. 13. Select geomorphic features in Norfolk Canyon (NC): (A) head and middle reaches of NC. Red dashed line represents axial incision: (1) is a short escarpment, (2) is an indentation of the canyon wall; both (1) and (2) are characteristic features of the southern rim of NC, (3) is a long, continuous step along NC's northern rim. (B) CHIRP profile across bathymetric platform in NC; the red dashed line is an unconformity that outcrops at a bathymetric platform. Group number of bathymetric step is explained in Section 4.5. (C) CHIRP profile across canyon axis illustrating axial incision, as well as evidence for lateral change in axial incision. (For interpretation of the references to color in this figure legend, the reader is referred to the web version of this article.)

Hanging valleys indicate differential rates of erosion between the primary canyon axis and tributary canyons, most likely due to enhanced erosion by sediment flows passing through the primary canyon during sea-level low-stands (e.g., Fig. 15). Alternatively, active transport of fluvial-sourced sediment down the main canyon axis may have continued during periods of early sea-level rise, while the tributary canyons, fed mostly by resuspended shelf sediment, may have shut down.

5.5. Evidence for recent and/or ongoing sediment transport

Although direct age constraints are not available, several fine-scale morphological observations suggest that some sediment transport has been active during the Holocene within the canyons studied. The intermittent v-shaped incisions we observed on the canyon floors have dimensions matching the fluidized debris flows described by Sanford et al. (1990), but the mechanism by which such flows are initiated remains unknown. Modern sediment transport in WiC has been studied using mid-range sidescan sonar (Mcgregor et al., 1982), bottom current meters (Sanford et al., 1990; Stanley, 1974), and direct seabed observations aboard submersibles (Mcgregor et al., 1982; Sanford et al., 1990; Stubblefield et al., 1982). These studies documented evidence for down-axis sediment transport, both in the nepheloid layer, particularly

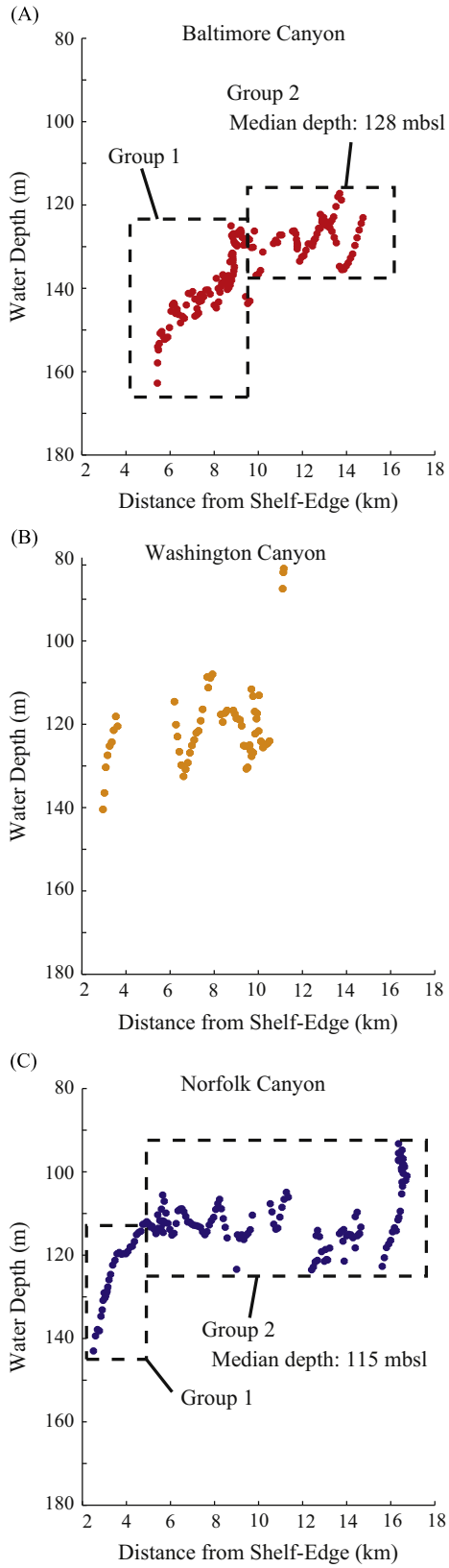

Fig. 14. Terrace depth versus absolute distance from the regional shelf-edge for (A) Baltimore Canyon, (B) Washington Canyon and (C) Norfolk Canyon. The upper edges of terraces were digitized and the depths were extracted at 100 m intervals.

during storm events, and along the canyon floor. Forde et al. (1981) observed intermittent current velocities between 20 and 30 cm/s at ~600 m water depth (3 m above the canyon floor) of WC and NC, corresponding to a range capable of entraining and transporting fine-grained sediments. Stubblefield et al. (1982) noted the outer (cut-bank) walls along thalweg meanders are steeper than the inner walls due to erosion and over-steepening induced by turbidity currents.

Although sediment cores along the axes of WC and NC indicate that sandy shelf sediment has entered the canyon head during the Holocene and has occasionally moved down-canyon, it is believed the canyons no longer funnel appreciable amounts of sediment to the deep sea (Forde et al., 1981; Knebel, 1984). Based on scree fields and talus piles along the canyon floor, Forde et al. (1981) proposed that the most active Holocene sediment transport toward the canyon axes in NC and WC involves periodic slope failures along steep canyon walls and gullies, but they were not able to identify specific failures or the extent of gravity-driven sediment transport. The spatial coincidence between increased steepness and roughness of sidewalls and increased variability of the thalweg gradient supports the notion that sediment transport down tributary canyons and gullies is recent and/or ongoing.

Surrounding the head of WC and one of its tributary canyons are a series of sediment waves that appear to spillover the canyon rim (Figs. 10A and B). The rounded bathymetric steps below the canyon rim suggest sediment transported over the rim has blanketed and smoothed pre-existing morphology. The sediment waves are comparable to large sand waves (2–9 m height and 100–600 m wavelength) on the shelf surrounding WiC that were inferred to be relic features, but continue to experience minor reworking (Knebel and Folger, 1976). Although we have no age control on the formation of the wave fields surrounding WC, it is possible they are active today and migrate during large storms.

6. Conclusions

The data and observations presented in this paper provide a first step towards characterizing the fine-scale geomorphic features within four major submarine canyons of the U.S. Atlantic Margin. Despite broad-scale morphologic similarities between the four canyons, we observe significant differences between their fine scale features, such as sinuosity, thalweg gradient, cross-canyon symmetry, and the density/roughness of side-wall gullies and tributary canyons. It appears that the general shape, orientation, and dominant geomorphic features of these canyons formed by processes no longer active today. The broad-scale morphology of tributary canyons and gullies may be closely tied to along-shore sediment transport during periods of lower sea-level, but Holocene modification to the canyon morphology is ongoing only within the confines of the canyons themselves. The following list summarizes our main conclusions: (1) canyon sinuosity and thalweg gradient may be a proxy for the frequency and/or grain-size of fluvial-sourced sediment flows passing through the canyons. (2) The spatial coincidence of the first major axial bend, drastic increase in variability of the thalweg gradient, and an increase in the density of sidewall gullies, scarps, scallops, and other morphologic features indicative of mass wasting may reflect the increasing importance of sediment transport orthogonal to the canyon axis closer to the shelf-edge. (3) Hanging valleys at the confluences of tributary canyons and the main canyons highlight the different erosion rates between sediment flows passing down the main canyon axis versus those sourced from tributaries. (4) Sediment waves trending into the head/north rim of WC, sediment draped across steps and terraces, and axial incisions along primary canyons each suggest some down-canyon sediment transport is ongoing; WC displays the most abundant evidence for recent activity. (5) Terraces mapped in all four canyons are likely relict features that have two origins: those centered ~120 m depth may represent a Late-Pleistocene paleoshoreline, whereas the

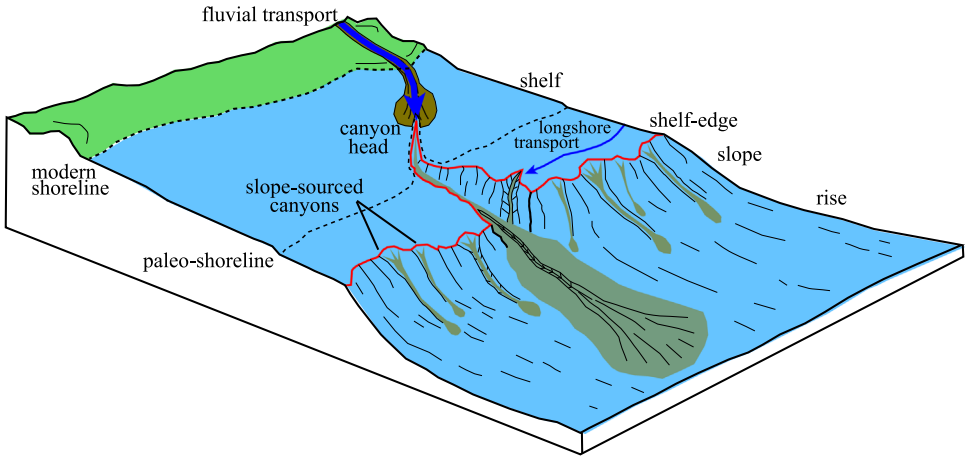

Fig. 15. Schematic depicting along and across shelf sediment sources during sea-level low-stands.

seaward dipping terraces form along lithological boundaries of outcropping shelf strata.

Acknowledgments

This project was funded by the U.S. Geological Survey (USGS), the U.S. Nuclear Regulatory Commission (Job Code: V6166) and the U.S Bureau of Ocean Energy Management (BOEM). CSA Ocean Sciences, Inc. is the contractor managing funding provided by BOEM. NOAA Office of Ocean Exploration and Research provided the *Nancy Foster* and *Okeanos Explorer* ship time. We thank Dr. A. W.J. Demopoulos (USGS) for facilitating USGS participation on the Nancy Foster cruise. We thank the crew and captain of the M/V *Tiki XIV*, NOAA ship *Okeanos Explorer*, the NOAA ship *Nancy Foster*, and the NOAA ship *Thomas Jefferson*. We particularly thank Captain Drexel "Stormy" Harrington, whose knowledge of the canyons was invaluable. We thank Chuck Worley, Eric Moore and Brian Andrews for support with data acquisition and processing. This paper benefitted greatly from reviews by Deborah Hutchinson and two anonymous reviewers. Mention of trade names does not imply U.S. Government endorsement of commercial products.

References

Andrews, B.D., Chaytor, J.D., ten Brink, U.S., Brothers, D.S., Gardner, J.V., 2013. Bathymetric Terrain Model of the Atlantic Margin for Marine Geological Investigations. U.S. Geological Survey Open-File Report 2012-1266, in press.
Brothers, D.S., ten Brink, U.S., Andrews, B.D., Chaytor, J.D., 2013a. Geomorphic characterization of the US Atlantic continental margin. Mar. Geol. 338, 46–63.
Brothers, D.S., ten Brink, U., Andrews, B., 2013b. Geomorphic process fingerprints in submarine canyons. Mar. Geol. 338, 46–63.
Butman, B., Twichell, D.C., Rona, P.A., Tucholke, B.E., Middleton, T.J., Robb, J.M., 2006. Seafloor Topography and Backscatter Intensity of the Hudson Canyon Region Offshore of New York and New Jersey. U.S. Geological Survey Open-File Report 2004-1411.
Cacchione, D.A., Pratson, L.F., Ogston, A.S., 2002. The shaping of continental slopes by internal tides. Science 296, 724–727.
Canals, M., Puig, P., de Madron, X.D., Heussner, S., Palanques, A., Fabres, J., 2006. Flushing submarine canyons. Nature 444, 354–357.
Catuneanu, O., 2006. Principles of Sequence Stratigraphy, 1st ed. Elsevier, Amsterdam.
Chaytor, J.D., ten Brink, U.S., Solow, A.R., Andrews, B.D., 2009. Size distribution of submarine landslides along the US Atlantic margin. Mar. Geol. 264, 16–27.
Colman, S.M., Halka, J.P., Hobbs, C.H., Mixon, R.B., Foster, D.S., 1990. Ancient channels of the Susquehanna River beneath Chesapeake Bay and the Delmarva Peninsula. Geol. Soc. Am. Bull. 102, 1268–1279.
Covault, J.A., Graham, S.A., 2010. Submarine fans at all sea-level stands: tectono-morphologic and climatic controls on terrigenous sediment delivery to the deep sea. J. Geol. 38, 939–942.
Farre, J.A., McGregor, B.A., Ryan, W.B.F., Robb, J.M., 1983. Breaching the shelfbreak: passage from youthful to mature phase in submarine canyon evolution. J. Sediment Res. A: Sediment. Petrol. Processes 33, 25–39.
Forde, E.B., 1981. Evolution of Veatch, Washington, and Norfolk submarine canyons – inferences from strata and morphology. Mar. Geol. 39, 197–214.
Forde, E.B., Stanley, D.J., Sawyer, W.B., Slagle, K.J., 1981. Sediment transport in Washington and Norfolk submarine canyons. Appl. Ocean Res. 3, 59–62.
Gardner, W.D., 1989a. Baltimore Canyon as a modern conduit of sediment to the deep-sea. Deep-Sea Res. Pt. 1-Oceanogr. Res. Pap. 36, 323–358.
Gardner, W.D., 1989b. Periodic resuspension in Baltimore Canyon by focusing of internal waves. J. Geophys. Res. 94, 18185–18194.
Goff, J.A., Austin Jr., J.A., Fulthorpe, C.S., 2013. Reinterpretation of the Franklin "Shore" in the Mid-Atlantic Bight as a Paleo-Shelf Edge. Cont. Shelf Res. 60, 64–69.
Hill, J.C., Driscoll, N.W., Weissel, J.K., Goff, J.A., 2004. Large-scale elongated gas blowouts along the US Atlantic margin. J. Geophys. Res., 109.
Kelling, G., Sheng, H., Stanley, D.J., 1975. Mineralogic composition of sand-sized sediment on outer margin off Mid-Atlantic states – assessment of influence of ancestral Hudson and other fluvial systems. Geol. Soc. Am. Bull. 86, 853–862.
Kelling, G., Stanley, D.J., 1970. Morphology and structure of Wilmington and Baltimore submarine canyons, Eastern United-States. J. Geol. 78, 637–660.
Kennett, J.P., 1982. Marine Geology. Prentice-Hall, Englewood Cliffs, NJ.
Knebel, H.J., 1984. Sedimentary processes on the Atlantic continental slope of the United States. Mar. Geol. 61, 43–74.
Knebel, H.J., Folger, D.W., 1976. Large sand waves on Atlantic outer continental-shelf around Wilmington Canyon, off Eastern United-States. Mar. Geol. 22, M7–M15.
Knebel, H.J., Spiker, E., 1977. Thickness and age of surficial sand sheet, Baltimore Canyon Trough area. Am. Assoc. Pet. Geol. Bull. 61, 861–871.
Lentz, S.J., 2008. Observations and a model of the mean circulation over the Middle Atlantic Bight continental shelf. J. Phys. Oceanogr 38, 1203–1221.
lo Iacono, C., Sulli, A., Agate, M., lo Presti, V., Pepe, F., Catalano, R., 2011. Submarine canyon morphologies in the Gulf of Palermo (Southern Tyrrhenian Sea) and possible implications for geo-hazard. Mar. Geophys. Res. 32, 127–138.
Mcgregor, B., Stubblefield, W.L., Ryan, W.B.F., Twichell, D.C., 1982. Wilmington Submarine Canyon – a marine fluvial-like system. J. Geol. 10, 27–30.
McGregor, B.A., Bennett, R.H., Lambert, D.N., 1979. Bottom processes, morphology, and geotechnical properties of the continental slope south of Baltimore Canyon. Appl. Ocean Res. 1, 177–187.
Micallef, A., Mountjoy, J.J., 2011. A topographic signature of a hydrodynamic origin for submarine gullies. J. Geol. 39, 115–118.
Mountain, G., Burger, R., Delius, H., Fulthorpe, C., Austin, J., Goldberg, D., Steckler, M.S., McHugh, C.M., Miller, K., Monteverde, D., Orange, D., Pratson, L., 2007. The Long-term Stratigraphic Record on Continental Margins. Blackwell Publishing, Malden, MA.
Mulder, T., Syvitski, J.P.M., 1995. Turbidity currents generated at river mouths during exceptional discharges to the world oceans. J. Geol. 103, 285–299.
Palanques, A., Puig, P., Latasa, M., Scharek, R., 2009. Deep sediment transport induced by storms and dense shelf-water cascading in the northwestern Mediterranean basin. Deep Sea Res. Pt. 1 Oceanogr. Res. Pap. 56, 425–434.
Palanques, A., Durrieu de Madron, X., Puig, P., Fabres, J., Guillén, J., Calafar, A., Canals, M., Heussner, S., Bonnin, J., 2006. Suspended sediment fluxes and transport processes in the Gulf of Lions submarine canyons. The role of storms and dense water cascading. Mar. Geol. 234, 43–61.
Palanques, A., Garcia-Ladona, E., Gomis, D., Martin, J., Marcos, M., Pascual, A., Puig, P., Gili, J.M., Emelianov, M., Monserrat, S., Guillen, J., Tintore, J., Segura, M., Jordi, A., Ruiz, S., Basterretxea, G., Font, J., Blasco, D., Pages, F., 2005. General patterns of circulation, sediment fluxes and ecology of the Palamo's (La Fonera) submarine canyon, northwestern Mediterranean. Prog. Oceanogr. 66, 89–119.
Paull, C.K., Caress, D.W., Ussler III, W., Lundsten, E., Meiner-Johnson, M., 2011. High-resolution bathymetry of the axial channels within Monterey and Soquel submarine canyons, offshore central California. Geosphere 7, 1077–1101.

Paull, C.K., Ussler, W., Greene, H.G., Keaten, R., Mitts, P., Barry, J., 2003. Caught in the act: the 20 December 2001 gravity flow event in Monterey Canyon. Geo-Mar. Lett. 22 (4), 227–232.
Peltier, W.R., Fairbanks, R.G., 2006. Global glacial ice volume and Last Glacial Maximum duration from an extended Barbados sea-level record. Quat. Sci. Rev. 25, 3322–3337.
Piper, D.J.W., Normark, W.R., 2001. Sandy fans – from Amazon to Hueneme and beyond. Am. Assoc. Pet. Geol. Bull. 85, 1407–1438.
Poag, C.W., 1992. U.S. Middle Atlantic Continental Rise: Provenance, Dispersal, and Deposition of Jurassic to Quaternary Sediments. Van Nostrand Reinhold, New York.
Popescu, I., Lericolais, G., Panin, N., Normand, A., Dinu, C., Le Drezen, E., 2004. The Danube submarine canyon (Black Sea): morphology and sedimentary processes. Mar. Geol. 206, 249–265.
Posamentier, H.W., Vail, P.R., 1988. Eustatic controls on clastic deposition II—sequence and systems tract models. In: Wilgus, C.K., Hastings, B.S., St.C. Kendall, C.G., Posamentier, H.W., Ross, C.A., Van Wagoner, J.C. (Eds.), Sea Level Changes—an Interated Approach. J. Sediment Res. Spec. Pub. 42, 125–154.
Pratson, L.F., Ryan, W.B.F., Mountain, G.S., Twichell, D.C., 1994. Submarine canyon initiation by downslope-eroding sediment flows: evidence in late Cenozoic strata on the New Jersey continental slope. Geol. Soc. Am. Bull. 106, 395–412.
Puig, P., Ogston, A.S., Mullenback, B.L., Nittrouer, C.A., Sternberg, R.W., 2003. Shelf-to-canyon sediment-transport processes on the Eel continental margin (northern California). Mar. Geol. 193, 129–149.
Rosgen, D.L., 1994. A classification of natural rivers. Catena 22, 169–199.
Sanford, M.W., Kuehl, S.A., Nittrouer, C.A., 1990. Modern sedimentary processes in the Wilmington Canyon area, United-States East Coast. Mar. Geol. 92, 205–226.
Shepard, F.P., 1981. Submarine canyons: multiple causes and long-time persistence. Am. Assoc. Pet. Geol. Bull. 65, 1062–1077.
Shepard, F.P., Marshall, N.F., McLoughlin, P.A., Sullivan, G.G., 1979. Currents in Submarine Canyons and other Sea Valleys. American Assocication of Petroleum Geologists, Tulsa, OK.
Stanley, D.J., Culver, S.J., Stubblefield, W.L., 1986. Petrologic and foraminiferal evidence for active downslope transport in Wilmington Canyon. Mar. Geol. 69, 207–218.
Stanley, D.J., Moore, G.T., 1983. The shelfbreak: critical interface on continental margins. J. Sediment Res. A: Sediment. Petrol. Processes 33, 233–250.
Stanley, D.J., 1974. Pebbly mud transport in head of Wilmington Canyon. Mar. Geol. 16, M1–M8.
Stubblefield, W.L., Mcgregor, B.A., Forde, E.B., Lambert, D.N., Merrill, G.F., 1982. Reconnaissance in DSRV Alvin of a fluvial-like meander system in Wilmington Canyon and slump features in South-Wilmington Canyon. J. Geol. 10, 31–36.
Thieler, R.E., Butman, B.B., Schwab, W.C., Allison, M.A., Driscoll, N.W., Donnelly, J.P., Uchupi, E., 2007. A catastrophic meltwater flood event and the formation of the Hudson Shelf Valley. Paleogeogr. Paleoclimatol. Paleoecol. 246, 120–136.
Twichell, D.C., Chaytor, J.D., ten Brink, U.S., Buczkowski, B., 2009. Morphology of late Quaternary submarine landslides along the US Atlantic continental margin. Mar. Geol. 264, 4–15.
Twichell, D.C., Grimes, C.B., Jones, R.S., Able, K.W., 1985. The role of erosion by fish in shaping topography around Hudson Submarine-Canyon. J. Sediment. Petrol. 55, 712–719.
Twichell, D.C., Roberts, D.G., 1982. Morphology, distribution, and development of submarine canyons on the United States Atlantic continental slope between Hudson arid Baltimore Canyons. J. Geol. 10, 408–412.
Twichell, D.C., Knebel, H.J., Folger, D.W., 1977. Delaware River – evidence for its former extension to Wilmington Submarine Canyon. Science 195, 483–485.
Xu, J.P., Swarzenski, P.W., Noble, M., Li, A., 2010. Event-driven sediment flux in Hueneme and Mugu submarine canyons, southern California. Mar. Geol. 269, 74–88.
Xu, J.P., Noble, M.A., Rosenfeld, L.K., 2004. In-situ measurements of velocity structure within turbidity currents. Geophys. Res. Lett. 31 (9).